

# Transition-Metal Ethene Bonds: Thermochemistry of $M^+(C_2H_4)_n$ ( $M = Ti-Cu$ , $n = 1$ and $2$ ) Complexes

M. R. Sievers, L. M. Jarvis,<sup>†</sup> and P. B. Armentrout\*

Contribution from the Department of Chemistry, University of Utah, Salt Lake City, Utah 84112

Received November 7, 1997

**Abstract:** Complexes of the first-row transition-metal cations ( $Ti^+-Cu^+$ ) with one and two ethene molecules are studied by guided ion beam mass spectrometry. Thermalized complexes are formed in a flow tube source and examined by energy-resolved collision-induced dissociation with Xe. The energy dependence of the CID cross sections is analyzed with consideration of multiple collisions, internal energy of the reactants, and lifetime effects. First,  $D_0(M^+-C_2H_4)$ , and second,  $D_0(C_2H_4M^+-C_2H_4)$ , adiabatic metal ion ethene bond energies, in eV, obtained in this study are  $1.51 \pm 0.11$  for Ti (first bond only),  $1.29 \pm 0.08$  and  $1.32 \pm 0.14$  for V,  $0.99 \pm 0.11$  and  $1.12 \pm 0.11$  for Cr,  $0.94 \pm 0.12$  and  $0.91 \pm 0.15$  for Mn,  $1.50 \pm 0.11$  and  $1.57 \pm 0.16$  for Fe,  $1.93 \pm 0.09$  and  $1.58 \pm 0.14$  for Co,  $1.89 \pm 0.11$  and  $1.79 \pm 0.15$  for Ni, and  $1.82 \pm 0.14$  and  $1.80 \pm 0.13$  for Cu, respectively. These values include corrections for diabatic dissociation in the cases of  $Fe^+(C_2H_4)$  and  $Mn^+(C_2H_4)_2$ , a point that is discussed in detail. Previous work obtained from theory and experiment is then compared with values determined in this study. Periodic trends observed for the mono- and bis-ethene complexes cations are also discussed and compared with the isobaric metal mono- and dicarbonyl cation complexes.

## Introduction

Studies of the interaction of ethene with metal centers are extensive. Hydrogenation of ethene using heterogeneous catalysts, such as Raney nickel and palladium on charcoal at elevated temperatures and high pressures, or homogeneous catalysts such as Wilkinson's catalyst,  $Rh(P\phi_3)_3Cl$ ,  $\phi = C_6H_5$ , have been studied.<sup>1</sup> Ziegler–Natta catalysts have been used to polymerize olefins rather efficiently.<sup>2,3,4</sup> The Wacker process deals with the conversion of olefins to aldehydes by transition metal catalysts.<sup>5</sup> The palladium analogue of Zeise's salt,  $Pt(C_2H_4)Cl_3^-$ , reacts with water to produce acetaldehyde.<sup>6</sup> A competitive channel to the Wacker process is hydroformylation, in which an alkene is converted into an aldehyde with one extra carbon (e.g., ethene is converted to propionaldehyde).<sup>7</sup> Exposition of the exact mechanism for many of these processes is still in progress, and certainly the thermochemistry and details of the potential energy surfaces involved have not been elucidated.

In the gas phase, a significant amount of work has been performed concerning the mechanisms and thermochemistry of the reactions of atomic transition-metal ions with hydrocarbons.<sup>8–13</sup> With alkanes larger than methane, a common product formed in these systems by dehydrogenation or alkane

elimination is  $M^+(C_2H_4)$ . To gain further insight into the mechanism of these reactions, the determination of the thermochemistry of these products is needed. Previous work has examined this thermochemistry for several late transition metals,<sup>9,14–31</sup> but little quantitative information is available for the early transition-metal ethene complexes.<sup>15,32–36</sup>

Other gas-phase studies, both experimental and theoretical, have centered on characterizing the bonding between metal ions

(10) Armentrout, P. B.; Beauchamp, J. L. *Acc. Chem. Res.* **1989**, *22*, 315.

(11) Armentrout, P. B. In *Selective Hydrocarbon Activation: Principles and Progress*; Davies, J. A., Watson, P. L., Liebman, J. F., Greenberg, A., Eds.; VCH: New York, 1990; pp 467–533.

(12) Van Koppen, P. A. M.; Brodbelt-Lustig, J.; Bowers, M. T.; Dearden, D. V.; Beauchamp, J. L.; Fisher, E. R.; Armentrout, P. B. *J. Am. Chem. Soc.* **1991**, *113*, 2359.

(13) Haynes, C. L.; Fisher, E. R.; Armentrout, P. B. *J. Am. Chem. Soc.* **1996**, *118*, 3269.

(14) Bohme, M.; Wagener, T.; Frenking, G. *J. Organomet. Chem.* **1996**, *520*, 31.

(15) Sodupe, M.; Bauschlicher, C. W. Jr.; Langhoff, S. R.; Partridge, H. *J. Phys. Chem.* **1992**, *96*, 2118.

(16) Perry, J. K. Ph.D. Thesis, Caltech, 1994.

(17) Hertwig, R. H.; Koch, W.; Schröder, D.; Schwarz, H.; Hrušák, J.; Schwerdtfeger, P. *J. Phys. Chem.* **1996**, *100*, 12253.

(18) Basch, H.; Hoz, T. Personal communication cited in ref 17.

(19) Fisher, E. R.; Armentrout, P. B. *J. Phys. Chem.* **1990**, *94*, 1680.

(20) Schultz, R. H.; Armentrout, P. B. Unpublished work.

(21) Schultz, R. H.; Elkind, J. L.; Armentrout, P. B. *J. Am. Chem. Soc.* **1988**, *110*, 411.

(22) Hanratty, M. A.; Beauchamp, J. L.; Illies, A. J.; van Koppen, P.; Bowers, M. T. *J. Am. Chem. Soc.* **1988**, *110*, 1.

(23) Jacobson, D. B.; Freiser, B. S. *J. Am. Chem. Soc.* **1983**, *105*, 5197.

(24) van Koppen, P. A. M.; Jacobson, D. B.; Illies, A. J.; Bowers, M. T.; Hanratty, M. A.; Beauchamp, J. L. *J. Am. Chem. Soc.* **1989**, *111*, 1991.

(25) van Koppen, P. A. M.; Bowers, M. T.; Beauchamp, J. L. *Organometallics* **1990**, *9*, 625.

(26) Jacobson, D. B.; Freiser, B. S. *J. Am. Chem. Soc.* **1983**, *105*, 7492.

(27) Jacobson, D. B.; Freiser, B. S. *J. Am. Chem. Soc.* **1983**, *105*, 736.

(28) Armentrout, P. B.; Beauchamp, J. L. *J. Am. Chem. Soc.* **1981**, *103*, 6628.

(29) Burnier, R. C.; Byrd, G. D.; Freiser, B. S. *Anal. Chem.* **1980**, *52*, 1641.

<sup>†</sup> NSF-REU participant. Present address: Department of Chemistry, Northwestern University, Evanston, IL 60208.

(1) Osborn, J. A.; Jardine, F. H.; Young, J. F.; Wilkinson, G. *J. Chem. Soc. A* **1966**, 1711.

(2) Ziegler, K.; Holzkamp, E.; Martin, H.; Breil, H. *Angew. Chem.* **1955**, *67*, 541. Natta, G. *J. Polym. Sci.* **1955**, *16*, 143.

(3) Sinn, H.; Kaminski, W. *Adv. Organomet. Chem.* **1980**, *18*, 99.

(4) Boor, J. *Ziegler–Natta Catalysis and Polymerizations*; Academic: New York, 1979.

(5) Parshall, G. W. *Science* **1980**, *208*, 1221.

(6) Backvall, J. E.; Åkermark, B.; Ljunggren, S. O. *J. Am. Chem. Soc.* **1979**, *101*, 2411.

(7) Tyler, D. R. *Prog. Inorg. Chem.* **1988**, *36*, 125. Pruettt, R. L. *J. Chem. Educ.* **1986**, *63*, 196.

(8) Armentrout, P. B. In *Gas-Phase Inorganic Chemistry*; Russell, D. H., Ed.; Plenum: New York, 1989; pp 1–42.

(9) Haynes, C. L.; Armentrout, P. B. *Organometallics* **1994**, *13*, 3480.

ligated by ethene and the related carbonyl molecule.<sup>15–18,37–45</sup> Qualitatively, the interactions of transition metals with such ligands can often be described by the Dewar–Chatt–Duncanson model.<sup>46</sup> In this model, the ligand donates electrons from its HOMO (the  $\pi$ -electrons of  $C_2H_4$  and the carbon lone pair of CO) into the  $\sigma$ -type metal orbitals. The metal then donates electrons from  $\pi$ -symmetry d orbitals into antibonding ligand orbitals (the  $\pi^*$  orbitals of  $C_2H_4$  and CO).

In this study, we use guided ion beam mass spectrometry to study the mono- and bis-ethene complexes of the first-row transition-metal cations (Ti–Cu) by collisionally dissociating the complex ions with xenon. The energy dependence of the collision-induced dissociation (CID) cross sections are interpreted to determine the 0 K bond dissociation energies (BDEs) of the metal ion–ethene bonds. The results are compared with literature values, both experimental and theoretical, in detail. The periodic trends in the bonding of metal ion–ethene and metal ion–bis-ethene complexes are examined and compared with those for the comparable metal ion carbonyls. This comparison reveals that for all metals but manganese the strength of the bonding interaction between the metal cation and the CO or  $C_2H_4$  ligand is nearly equivalent. This study provides the first systematic experimental study examining the BDEs for the entire first-row transition-metal series with one and two ethene molecules. We also compare the periodic trend in BDEs between the first-row transition-metal cations ligated with  $C_2H_4$  and CO (both  $\sigma$ -donor and  $\pi$ -acceptor),  $NH_3$  ( $\sigma$ -donor), and  $H_2O$  ( $\sigma$ -donor and  $\pi$ -donor). This comparison shows that the  $\pi$ -back-bonding that occurs between the metal and the ethene ligand enhances the BDEs significantly as you go from the early to the late metals.

## Experimental Section

These studies are performed using a guided ion beam tandem mass spectrometer. The instrument and experimental methods have been described previously.<sup>47,48</sup> Ions, formed as described below, are extracted from the source, accelerated, and focused into a magnetic sector momentum analyzer for mass analysis. The ions are decelerated to a desired kinetic energy and focused into an octopole ion guide that

radially traps the ions. While in the octopole, the ions pass through a gas cell that contains the neutral reactant at pressures where multiple collisions are improbable (<0.30 mTorr). The product ions and the reactant ion beam drift out of the gas cell, are focused into a quadrupole mass filter, and then are detected by a secondary electron scintillation detector.

Ion intensities are converted to absolute cross sections as described previously.<sup>47</sup> Uncertainties in the absolute cross sections are estimated at  $\pm 20\%$ . To determine the absolute zero and distribution of the ion kinetic energy, the octopole is used as a retarding energy analyzer.<sup>47</sup> The uncertainty in the absolute energy scale is  $\pm 0.05$  eV (lab). The full width at half-maximum (fwhm) of the ion energy distribution is  $\sim 0.3$  eV (lab). Lab energies are converted into center-of-mass energies by using the formula  $E(CM) = E(lab) m/(m + M)$  where  $M$  and  $m$  are the masses of the ion beam and neutral reactant, respectively. All energies stated in this paper are in the center-of-mass frame.

**Ion Source.** The ion source, described in previous work,<sup>48</sup> utilizes a direct current discharge source utilizing a cathode made of the desired metal for Ti, V, Cr, Fe, Co, Ni, and Cu. For Mn, chunks of manganese are held in a tantalum boat cathode. The cathode is held at 1.5–3 kV and has a flow of approximately 90% He and 10% Ar passing over it at a typical pressure of  $\sim 0.5$  Torr.  $Ar^+$  ions created in the discharge are accelerated toward the metal cathode, sputtering atomic metal ions. In the flow tube,  $\sim 2$  mTorr of ethene gas is introduced 50 cm downstream of the discharge to produce the mono- and bis-ligated complexes by three-body stabilization. The ions then undergo  $\sim 10^5$  collisions with He and  $\sim 10^4$  collisions with Ar in the meter long flow tube before entering the guided ion beam apparatus. These collisions are sufficient to form the desired complexes by three-body stabilization and to thermalize the complexes. Previous work performed under similar conditions<sup>40,42,49,50,51</sup> indicates that the internal temperature of metal–ligand complexes formed in the flow tube is generally near 300 K.

In the case of  $Ti^+$ , which has a strong affinity to dehydrogenate hydrocarbons,<sup>52,53</sup> ethane gas was used to generate the mono-ethene complex. Several different means of producing the titanium bis-ethene complex were attempted, but none provided sufficiently intense beams for study. The inability to form the bis-ethene complex of  $Ti^+$  is supported by the studies of Guo and Castleman.<sup>53</sup> They observed that when  $Ti^+$  was exposed to ethene in a flow tube, the only bis-complexes formed were  $(C_2H_2)Ti^+(C_2H_4)$  and small amounts of  $Ti^+(C_2H_2)_2$ .

The major isotope (56 amu) of iron has the same nominal mass as two ethene molecules (28 amu each). If excessive amounts of ethene are admitted to the flow tube, intense beams of ethene clusters,  $(C_2H_4)_x^+$ , having the same nominal mass as the mono- and bis-ligated iron complex, can be generated. Studies with  $^{54}Fe$  complexes verified that the cross sections obtained for  $^{56}Fe$  complexes correspond to the desired iron–ligand system. Care was also taken in the case of the manganese complexes, where the desired mass differs by only a single mass unit from ethene clusters. In this case, the difficulty stems from the inability to generate intense beams of the desired manganese complexes under conditions where ethene cluster formation is also suppressed. Careful attention to the mass of the reactants and to residual mass overlap with the ethene clusters verifies that the cross sections obtained in this study correspond to  $Mn(C_2H_4)_n^+$  species.

To verify further that  $(C_2H_4)_x^+$  CID products were not contributing to the cross sections that we obtained for  $Fe^+(C_2H_4)_n^+$  and  $Mn^+(C_2H_4)_n^+$ , where  $n = 1$  and 2, we performed CID experiments on the ethene cluster cations. The ethene trimer cation is observed to lose  $C_2H_4$  inefficiently, such that interference with the  $Fe^+$  product from  $Fe^+(C_2H_4)$  is improbable. However,  $C_2H_3$  loss from the trimer does form a product that could interfere with the  $Mn^+$  product from  $Mn^+(C_2H_4)$ , but this

(30) van Koppen, P. A. M.; Bowers, M. T.; Beauchamp, J. L.; Dearden, D. V. *ACS Symp. Ser.* **1990**, 428, 34.

(31) Sievers, M. R.; Armentrout, P. B. Unpublished results.

(32) Sunderlin, L. S.; Armentrout, P. B. *J. Am. Chem. Soc.* **1989**, 111, 3845.

(33) Sunderlin, L. S.; Armentrout, P. B. *Int. J. Mass Spectrom. Ion Processes* **1989**, 94, 149.

(34) Aristov, N.; Armentrout, P. B. *J. Am. Chem. Soc.* **1986**, 108, 1806.

(35) Georgiadis, R.; Armentrout, P. B. *Int. J. Mass Spectrom. Ion Processes* **1989**, 89, 227.

(36) Hanton, S. D.; Sanders, L.; Weisshaar, J. C. *J. Phys. Chem.* **1989**, 93, 1963.

(37) Barnes, L. A.; Rosi, M.; Bauschlicher, C. W., Jr. *J. Chem. Phys.* **1990**, 93, 609.

(38) Meyer, F.; Armentrout, P. B. *Mol. Phys.* **1996**, 88, 187.

(39) Sievers, M. R.; Armentrout, P. B. *J. Phys. Chem.* **1995**, 99, 8135.

(40) Khan, F. A.; Clemmer, D. E.; Schultz, R. H.; Armentrout, P. B. *J. Phys. Chem.* **1993**, 97, 7978.

(41) Khan, F. A.; Armentrout, P. B. Unpublished work.

(42) Schultz, R. H.; Crellin, K. C.; Armentrout, P. B. *J. Am. Chem. Soc.* **1991**, 113, 8590.

(43) Goebel, S.; Haynes, C. L.; Khan, F. A.; Armentrout, P. B. *J. Am. Chem. Soc.* **1995**, 117, 6994.

(44) Khan, F. A.; Steele, D. A.; Armentrout, P. B. *J. Phys. Chem.* **1995**, 99, 7819.

(45) Meyer, F.; Chen, Y.-M.; Armentrout, P. B. *J. Am. Chem. Soc.* **1995**, 117, 4071.

(46) Dewar, M. J. S. *Bull. Soc. Chim. Fr.* **1951**, 18, C79. Chatt, J.; Duncanson, L. A. *J. Chem. Soc.* **1953**, 2939.

(47) Ervin, K. M.; Armentrout, P. B. *J. Chem. Phys.* **1985**, 83, 166.

(48) Schultz, R. H.; Armentrout, P. B. *Int. J. Mass Spectrom. Ion Processes* **1991**, 107, 29.

(49) Schultz, R. H.; Armentrout, P. B. *J. Chem. Phys.* **1992**, 96, 1046.

(50) Dalleska, N. F.; Honma, K.; Armentrout, P. B. *J. Am. Chem. Soc.* **1993**, 115, 12125.

(51) Dalleska, N. F.; Honma, K.; Sunderlin, L. S.; Armentrout, P. B. *J. Am. Chem. Soc.* **1994**, 116, 3519.

(52) Sunderlin, L. S.; Armentrout, P. B. *Int. J. Mass Spectrom. Ion Processes* **1989**, 94, 149.

(53) Guo, B. C.; Castleman, A. W., Jr. *J. Am. Chem. Soc.* **1992**, 114, 6152; *J. Am. Soc. Mass Spectrom.* **1992**, 3, 464; *Int. J. Mass Spectrom. Ion Processes* **1992**, 112, R1.

**Table 1.** Reactant Vibrational Frequencies

| M                  | complex  | frequencies (cm <sup>-1</sup> )   |
|--------------------|--|---|
| Ti–Mn <sup>a</sup> | M <sup>+</sup> (C <sub>2</sub> H <sub>4</sub> )              | 272, 292, 538, 801, 841, 903, 982, 1167, 1206, 1427, 1505, 2934, 2947, 3003, 3024 |
|                    | M <sup>+</sup> (C <sub>2</sub> H <sub>4</sub> ) <sub>2</sub> | 50, 75, 100 + 2 M <sup>+</sup> (C <sub>2</sub> H <sub>4</sub> ) frequencies       |
| Fe–Cu <sup>b</sup> | M <sup>+</sup> (C <sub>2</sub> H <sub>4</sub> )              | 307, 354, 519, 791, 902, 969, 978, 1144, 1198, 1374, 1459, 2921, 2926, 3008, 3024 |
|                    | M <sup>+</sup> (C <sub>2</sub> H <sub>4</sub> ) <sub>2</sub> | 50, 75, 100 + 2 M <sup>+</sup> (C <sub>2</sub> H <sub>4</sub> ) frequencies       |

<sup>a</sup> Reference 56. <sup>b</sup> Reference 57. These frequencies have been scaled by 0.94 as discussed in the text.

reaction has a higher apparent threshold than that of the Mn<sup>+</sup> product such that any contamination should not cause a problem with the threshold determination. The ethene tetramer cation does not lose C<sub>2</sub>H<sub>4</sub> such that no interference with the Fe<sup>+</sup>(C<sub>2</sub>H<sub>4</sub>) product from Fe<sup>+</sup>(C<sub>2</sub>H<sub>4</sub>)<sub>2</sub> occurs. This cluster does lose C<sub>2</sub>H<sub>5</sub> to form a C<sub>6</sub>H<sub>11</sub><sup>+</sup> product with a slightly lower threshold than that for the isobaric Mn<sup>+</sup>(C<sub>2</sub>H<sub>4</sub>) product from Mn<sup>+</sup>(C<sub>2</sub>H<sub>4</sub>)<sub>2</sub>. To ensure the identity of the manganese complex, the pressure of ethene in the flow tube was adjusted until no C<sub>6</sub>H<sub>11</sub><sup>+</sup> was observed.

**Threshold Analysis.** The threshold regions of the cross sections are analyzed using eq 1,

$$\sigma(E) = \sigma_0 \sum g_i (E + E_{\text{rot}} + E_i - E_0)^n / E \quad (1)$$

where  $\sigma_0$  is an energy-independent scaling parameter,  $E$  is the relative collisional energy,  $E_{\text{rot}}$  is the rotational energy of the reactants,  $E_0$  is the reaction threshold at 0 K, and  $n$  is an adjustable parameter. The summation is over all vibrational states having populations  $g_i$  ( $\sum g_i = 1$ ) and energies  $E_i$ . The rotational energy distribution is relatively narrow with the average rotational energy of the ions being  $3kT/2 = 0.039$  eV at  $T = 300$  K.

This equation has been shown to be useful in the interpretation of many cross sections of endothermic processes.<sup>40,42</sup> Details about the implementation of eq 1 in determining thresholds is described elsewhere.<sup>42,47</sup> Briefly, the Beyer–Swinehart algorithm<sup>54</sup> is used to evaluate the density of the ion vibrational states, and then the relative populations  $g_i$  are calculated by the appropriate Maxwell–Boltzmann distribution at 300 K. Last, we use RRKM theory in a procedure described<sup>40,55</sup> to examine explicitly lifetime effects on thresholds. This effect was found to be insignificant for all complex ions studied.

No experimental measurements of the vibrational frequencies of transition-metal cation–ethene complexes exist. Theoretical studies have calculated vibrational frequencies for M<sup>+</sup>(C<sub>2</sub>H<sub>4</sub>) where M = Ti,<sup>56</sup> Co,<sup>57</sup> Ni, and Cu.<sup>58</sup> For M = Ti–Mn, the frequencies calculated in the former study of Ti<sup>+</sup>(C<sub>2</sub>H<sub>4</sub>) were used, while those from Bärtsch and Schwarz on Co<sup>+</sup>(C<sub>2</sub>H<sub>4</sub>) were used for M = Fe–Cu. The latter set of frequencies were scaled by 0.94,<sup>59</sup> a factor that makes the average C–H stretching frequencies equal those calculated for Ti<sup>+</sup>(C<sub>2</sub>H<sub>4</sub>). The frequencies used for all metal ion–ethene complexes are given in Table 1. For the bis-ligated complexes, nine frequencies in addition to the ethene vibrations are required. Six of these are obtained by doubling the degeneracies of the frequencies used in the monoligated complex. Three additional frequencies are estimates based on deformation modes of previously determined transition-metal dicarbonyl cation complexes.<sup>40</sup> To estimate the uncertainty introduced by the unknown frequencies used in our analyses, we also interpret our data using metal–ligand

(54) Beyer, T.; Swinehart, D. F. *Comm. Assoc. Comput. Machines* **1973**, 379. Stein, S. E.; Rabinovitch, B. S. *J. Chem. Phys.* **1973**, 58, 2438; *Chem. Phys. Lett.* **1977**, 49, 183. Gilbert, R. G.; Smith, S. C. *Theory of Unimolecular and Recombination Reactions*; Blackwell Scientific: Oxford, U.K., 1990.

(55) Rodgers, M. T.; Ervin, K. M.; Armentrout, P. B. *J. Chem. Phys.* **1997**, 106, 4499.

(56) Jensen, V. R.; Børve, K. J.; Westberg, N.; Ystenes, M. *Organometallics* **1995**, 14, 4349.

(57) Bärtsch, S.; Schwarz, H. Personal communication.

(58) Hertwig, R. H.; Koch, W. Unpublished results.

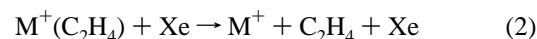
(59) If the frequencies calculated by Bärtsch and Schwarz for free ethene are compared with experimental frequencies, a scaling factor of 0.96 is obtained. These two factors (0.94 and 0.96) lead to differences in the internal energy of a metal ethene complex of only ~1.3 meV.

frequencies in Table 1 scaled by factors of 0.8 and 1.2, such that three sets of frequencies are considered.

Before comparison with the experimental data, the model cross section of eq 1 is convoluted over the ion and neutral energy distributions as described previously.<sup>47</sup> The  $\sigma_0$ ,  $n$ , and  $E_0$  parameters of eq 1 are then optimized using a nonlinear least-squares analysis to best reproduce the data. All acceptable fits were used to determine mean values for  $\sigma_0$ ,  $E_0$ , and  $n$ . Reported  $E_0$  values are the mean obtained from analyses using the three sets of frequencies with errors that reflect these uncertainties. The stated errors also reflect the spread in  $E_0$  values determined from different data sets obtained on different days and also the uncertainty of the energy scale, 0.05 eV (lab).

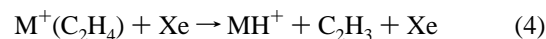
## Results

**M<sup>+</sup>(C<sub>2</sub>H<sub>4</sub>) + Xe.** Results for the reaction of V(C<sub>2</sub>H<sub>4</sub>)<sup>+</sup> and Cu<sup>+</sup>(C<sub>2</sub>H<sub>4</sub>) with Xe are shown in Figure 1. The M<sup>+</sup> product ion channels shown in Figure 1 are representative of those observed for all monoligated metal complexes studied here. The primary product ion observed is the atomic metal ion, corresponding to loss of the ligand, reaction 2. This process has an apparent threshold near 1 eV and reaches a relatively constant magnitude above ~5 eV. For M = V, Fe, Co, Ni, and Cu, MXe<sup>+</sup> is also formed by ligand exchange, reaction 3, at low energies. The ligand exchange product, MXe<sup>+</sup>, has an apparent

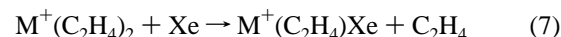
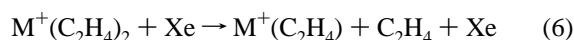


threshold near 1 eV. The peak of the ligand exchange channel occurs as the cross section for the ligand loss channel, reaction 2, rises steeply. This behavior clearly indicates a strong competition between the two processes. For Ti<sup>+</sup>, Cr<sup>+</sup>, and Mn<sup>+</sup>, the MXe<sup>+</sup> product is not observed, presumably because its magnitude is too small for our experimental conditions, <0.1 Å<sup>2</sup>.

At higher energies, additional products were observed for several metal complexes as shown in reactions 4 and 5. The collision-induced dissociation of M<sup>+</sup>(C<sub>2</sub>H<sub>4</sub>) with Xe resulted in the formation of MH<sup>+</sup> for M = Ti, Cr, Fe, Co, and Ni and MCH<sub>2</sub><sup>+</sup> with M = Ti, V, Fe, Co, Ni, and Cu. The MH<sup>+</sup> cross sections have apparent thresholds near 5 eV and then rise to maxima that are usually an order of magnitude lower than the simple ligand loss channels. The MCH<sub>2</sub><sup>+</sup> cross sections have apparent thresholds that are near 7 eV and reach maximum cross section magnitudes near 0.1 Å<sup>2</sup>.



**M<sup>+</sup>(C<sub>2</sub>H<sub>4</sub>)<sub>2</sub> + Xe.** Results for the collision-induced dissociation of V<sup>+</sup>(C<sub>2</sub>H<sub>4</sub>)<sub>2</sub> and Cu<sup>+</sup>(C<sub>2</sub>H<sub>4</sub>)<sub>2</sub> with Xe are shown in Figure 2. The product ion channels shown are representative of those observed for all metals studied here. The major product ion observed is that resulting from the loss of one C<sub>2</sub>H<sub>4</sub> ligand, M<sup>+</sup>(C<sub>2</sub>H<sub>4</sub>), in reaction 6. Its cross section rises from an apparent threshold near 0.5–1 eV and reaches a relatively constant magnitude above ~3 eV. As also seen in the monoligated systems discussed above, the next most abundant product ion is that produced by ligand exchange, reaction 7. The ligand



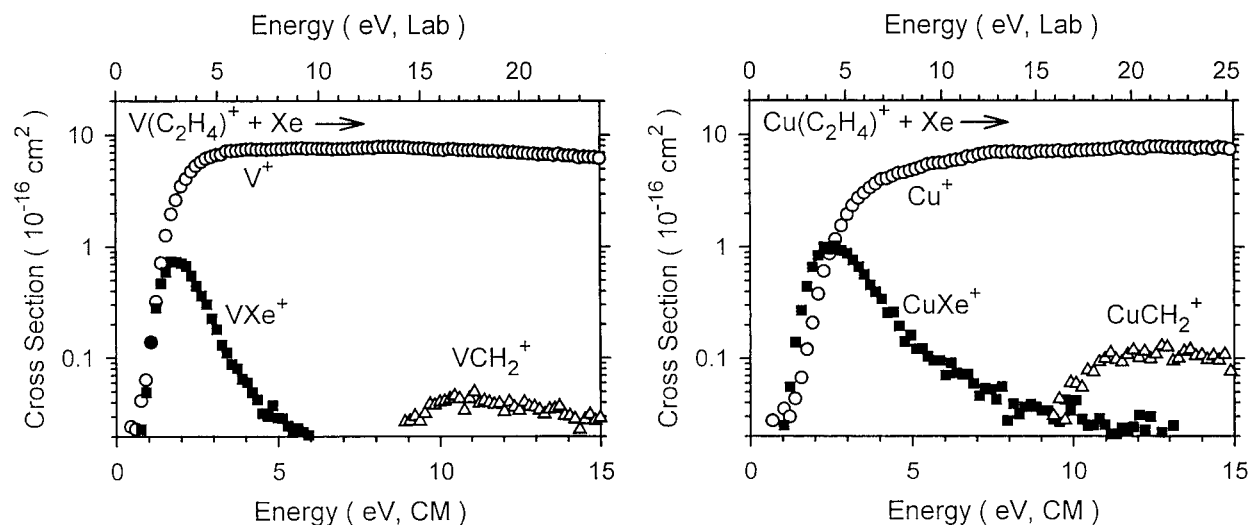


**Figure 1.** Cross sections for the collision-induced dissociation of  $M^+(C_2H_4)$  with Xe as a function of relative kinetic energy ( $x$ -axis) to form  $M^+$  (circles),  $MXe^+$  (squares), and  $MCH_2^+$  (triangles). Part a (left) shows results for  $M = V$  while part b (right) shows data for  $M = Cu$ .

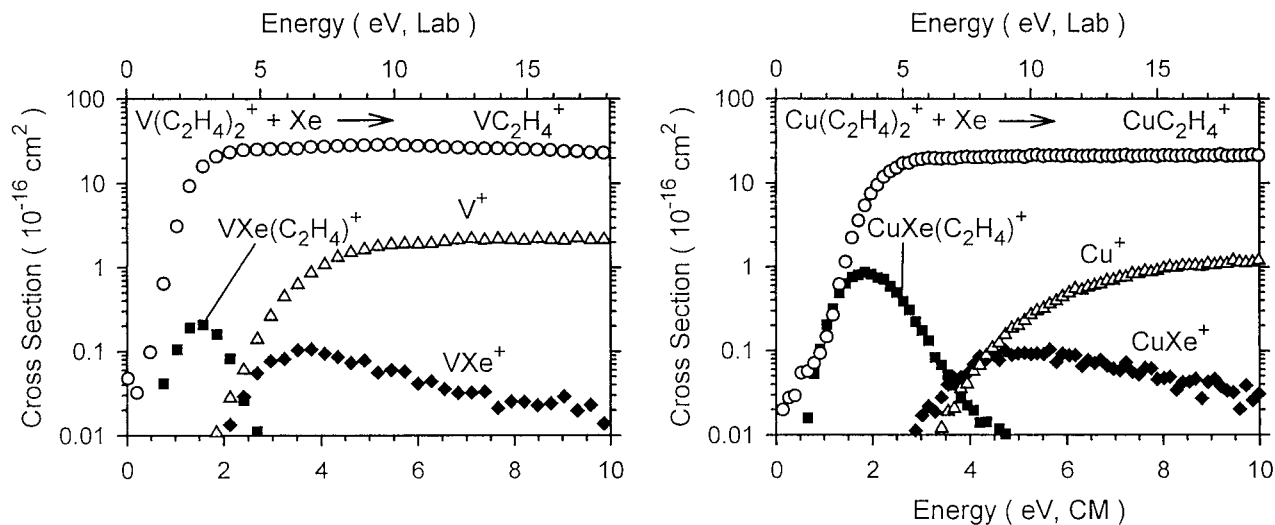
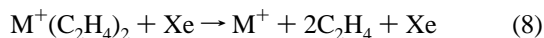


**Figure 2.** Zero-pressure extrapolated cross sections for the collision-induced dissociation of  $M^+(C_2H_4)_2$  with Xe as a function of relative kinetic energy ( $x$ -axis) to form  $M^+(C_2H_4)$  (circles),  $M^+(C_2H_4)Xe$  (squares),  $M^+$  (triangles), and  $MXe^+$  (diamonds). Part a (left) shows results for  $M = V$  while part b (right) shows data for  $M = Cu$ .

exchange product,  $M^+(C_2H_4)Xe$ , observed for  $M = V, Fe, Co, Ni,$  and  $Cu$ , has an apparent threshold of 0.5–1 eV and a peak that occurs near the apparent threshold of the ligand loss cross section, again demonstrating a competition between ligand loss and ligand exchange. The collision-induced dissociation of the bis-ethene metal complex yields no products comparable to those formed in reactions 4 and 5.

At the energy that the ligand loss channel starts to level out, the  $M^+$  channel for all metal cations starts to rise because of reaction 8, sequential dissociation of the second ethene ligand. These channels have apparent thresholds near 2 to 4



eV and rise to maxima that are usually an order of magnitude or so smaller than the simple ligand loss channel. Similar thresholds are obtained for the ligand exchange processes 9.

**Threshold Analysis.** The product ion cross sections for reactions 2 and 6, CID of  $M^+(C_2H_4)$  and  $M^+(C_2H_4)_2$ , were analyzed using eq 1. The optimized parameters are listed in

**Table 2.** Optimized Parameters for Eq 1

| M  | $n$           | $\sigma_0$      | $E_0, eV$       |
|--|---------------|-----------------|-----------------|
| $M^+(C_2H_4) + Xe \rightarrow M^+ + C_2H_4 + Xe$           |               |                 |                 |
| Ti   | $1.5 \pm 0.4$ | $8.0 \pm 0.7$   | $1.51 \pm 0.11$ |
| V  | $1.6 \pm 0.2$ | $8.3 \pm 0.8$   | $1.29 \pm 0.08$ |
| Cr   | $1.9 \pm 0.4$ | $6.4 \pm 1.3$   | $0.99 \pm 0.11$ |
| Mn   | $2.9 \pm 0.4$ | $2.9 \pm 1.0$   | $0.94 \pm 0.12$ |
| Fe   | $1.5 \pm 0.3$ | $5.5 \pm 1.3$   | $1.73 \pm 0.11$ |
| Co   | $1.7 \pm 0.2$ | $4.4 \pm 0.8$   | $1.93 \pm 0.09$ |
| Ni   | $1.9 \pm 0.2$ | $3.4 \pm 1.1$   | $1.89 \pm 0.11$ |
| Cu   | $2.0 \pm 0.3$ | $3.4 \pm 0.9$   | $1.82 \pm 0.14$ |
| $M^+(C_2H_4)_2 + Xe \rightarrow M^+(C_2H_4) + C_2H_4 + Xe$ |               |                 |                 |
| V  | $1.1 \pm 0.2$ | $70.8 \pm 19.1$ | $1.32 \pm 0.14$ |
| Cr   | $1.5 \pm 0.3$ | $47.0 \pm 6.7$  | $1.12 \pm 0.11$ |
| Mn   | $1.5 \pm 0.3$ | $70.0 \pm 9.1$  | $1.91 \pm 0.11$ |
| Fe   | $1.7 \pm 0.4$ | $31.8 \pm 9.5$  | $1.57 \pm 0.16$ |
| Co   | $1.9 \pm 0.4$ | $29.6 \pm 6.2$  | $1.58 \pm 0.14$ |
| Ni   | $1.6 \pm 0.5$ | $35.9 \pm 7.2$  | $1.79 \pm 0.15$ |
| Cu   | $1.5 \pm 0.4$ | $41.2 \pm 5.4$  | $1.80 \pm 0.13$ |

Table 2. We carefully examined whether the CID product cross sections were influenced by the pressure of the neutral collision gas because excessively high pressures can lead to multiple collisions that lower the thresholds measured. For the mono-

ethene complexes, we found no noticeable dependence of the cross sections on pressure, but for the bis-ethene complexes, the effect of pressure was noticeable. In these cases, the cross sections are extrapolated to zero neutral pressure, rigorously single collision conditions, as described previously.<sup>60</sup> Threshold analyses of the CID cross sections for the bis-ethene complexes were performed only on the zero pressure extrapolated cross sections.

In the mono-ethene complexes for  $M = V, Cr,$  and  $Fe-Cu$  and the bis-ethene complexes for  $M = Ni$  and  $Cu$ , a low-energy feature was observed in the ligand loss channel. These features are much smaller than the dominant cross section feature ( $<1\%$  in all cases) and generally distinct. Similar low-energy features have been observed in previous CID studies of metal–ligand cation complexes<sup>9,13,61</sup> and attributed to the formation of metastable excited states of the complexes. These features clearly complicate the analysis of the cross sections, and hence we follow the protocol established in previous work.<sup>61</sup> In the present study, the cross sections were initially analyzed disregarding the low-energy feature. Then the cross section was analyzed by reproducing the data with the sum of two models, one for the low-energy feature and one for the dominant high-energy feature. Several possible models for the low-energy feature were considered, and this is reflected in the uncertainty in the thresholds listed in Table 2. Thresholds obtained by ignoring the low-energy feature are lower (by approximately 0.1–0.2 eV) than those obtained with the two-model approach and have a corresponding value for the parameter  $n$  in eq 1 that is higher, reflecting an apparently slower rise in the threshold. As in our previous work,<sup>61</sup> we believe that the BDEs taken from the analyses that include explicit consideration of the low-energy feature provide the more accurate assessment of the BDEs of the complexes. These values are reported in Table 2.

Because all sources of reactant energy are accounted for in our data analysis, the thresholds tabulated in Table 2 should correspond to 0 K values. Threshold energies determined for CID processes can be converted into BDEs by assuming that the measured  $E_0$  values are the energy differences between the reactant and product energy asymptotes. This assumption has been shown to be valid for most ion–molecule reactions,<sup>62,63</sup> and theoretical considerations also demonstrate it should be true for simple heterolytic bond fission.<sup>64</sup> One potential ambiguity in the interpretation of the CID thresholds is whether they refer to diabatic (spin-conserving) or adiabatic (spin-changing) bond fission processes. On the basis of theoretical calculations of the  $M^+(C_2H_4)$  complexes,<sup>15</sup> the ground electronic states have the same spin state as that of the atomic metal ion except in the cases of  $M = Ti$  and  $Fe$ . We have discussed the case of  $Fe$  previously<sup>65</sup> and concluded from comparisons with other data that CID of  $Fe^+(C_2H_4)$  with  $Xe$  induces diabatic dissociation, similar to our conclusion for  $Fe^+(CO)$ .<sup>42</sup> If this hypothesis is correct, the true adiabatic BDE is obtained by reducing the threshold measured here by the  $^4F-^6D$  excitation energy, 0.23

eV.<sup>66</sup> In the case of  $Ti$ , similar considerations indicate that the  $Ti^+(C_2H_4)$  complex dissociates adiabatically and therefore needs no adjustment (which in this case would be a reduction of 0.57 eV,<sup>66</sup> the  $^2F-^4F$  excitation energy). Both of these conclusions are reexamined and verified in the discussion below.

Less information is available to consider this question for the bis-ethene–metal cation complexes. For most of the metals, the situation is fairly clear. The first ethene ligand induces a spin change for  $Ti^+$  and  $Fe^+$ , such that these  $M^+(C_2H_4)_2$  complexes almost certainly have the same spin state as  $M^+(C_2H_4)$ . For  $Ni$  and  $Cu$  complexes (doublet and singlet, respectively), no spin change is possible, and it is highly unlikely for the  $Co$  (triplet) system. Sodupe et al.<sup>15</sup> find excitation energies of 0.64, 2.12, and 1.00 eV for the low spin states of  $V^+(C_2H_4)$ ,  $Cr^+(C_2H_4)$ , and  $Mn^+(C_2H_4)$  such that a second ethene ligand can plausibly induce a spin change for vanadium and manganese, but not for chromium. In the analogous carbonyl complexes, calculations find that the ground states for  $M^+(CO)_2$  complexes ( $M = Ti-Cu$ ) differ in spin multiplicity from the  $M^+(CO)$  complexes only for  $M = Mn$ , where the excitation energy is 0.75 eV.<sup>37</sup> Therefore, the possibility that  $V^+(C_2H_4)_2$  and  $Mn^+(C_2H_4)_2$  have triplet and quintet ground states, respectively, should be explicitly considered and is discussed below.

**Minor Products.** Formation of  $MH^+$  and  $MCH_2^+$  products, which are the result of activation of a C–H or C–C bond of ethene, is much less efficient than the simple ligand loss. Simple analysis of these cross sections with eq 1 generally yields thresholds in excess of the thermodynamic thresholds for formation of these products. The cross sections can be modeled with  $E_0$  values consistent with the established metal–hydride cation and metal–carbene cation BDEs,<sup>65</sup> but the values needed for the parameter  $n$  were large. These observations indicate that the reactions are suppressed by competition with the much more favorable CID process. This behavior has been observed and discussed more fully for CID processes of other alkene–ligated transition-metal cations.<sup>9,13</sup>

## Discussion

**Bond Energies for  $M^+(C_2H_4)$ .** (1) **Comparison with Theory.** The accuracy of our results can be evaluated by comparing the individual bond dissociation energies (BDEs) for  $M^+(C_2H_4)$  obtained in this study with those derived from the ab initio calculations. The most systematic study is that of Sodupe, Bauschlicher, Langhoff, and Partridge (SBLP),<sup>15</sup> who examined  $M = Sc-Cu$ . In their work, the geometry of the complexes was optimized at the SCF level of theory. Using the SCF optimized geometry, the  $D_e$  values were then calculated at a higher level of theory, MCPF. These bond energies are listed in Table 3 after adjusting to  $D_0$  values.<sup>67</sup> SBLP estimated in their study that the reported BDEs could increase by  $0.35 \pm 0.04$  eV for  $Ti^+(C_2H_4)$  and  $0.17 \pm 0.04$  eV for  $M^+(C_2H_4)$  where  $M = V-Cu$  if larger basis sets and improved electron correlation were used. These adjustments to the theoretical values have been recently tabulated (rounded to the nearest kcal/mol)<sup>68</sup> and are also listed in Table 3.

A comparison of the theoretical values with our experimental values, Table 3, shows that the former are systematically lower. The directly calculated  $D_0$  values lie an average of  $0.31 \pm 0.14$

(60) Hales, D. A.; Lian, L.; Armentrout, P. B. *Int. J. Mass Spectrom. Ion Processes* **1990**, *102*, 269.

(61) Meyer, F.; Khan, F. A.; Armentrout, P. B. *J. Am. Chem. Soc.* **1995**, *117*, 9740.

(62) Armentrout, P. B. In *Advances in Gas-Phase Ion Chemistry*; Adams, N. G., Babcock, L. M., Eds.; JAI: Greenwich, 1992; Vol. 1, pp 83–119.

(63) Boo, B. H.; Armentrout, P. B. *J. Am. Chem. Soc.* **1987**, *109*, 3459. Ervin, K. M.; Armentrout, P. B. *J. Phys. Chem.* **1987**, *86*, 2659. Elkind, J. L.; Armentrout, P. B. *J. Phys. Chem.* **1984**, *88*, 5454. Armentrout, P. B. In *Structure/Reactivity and Thermochemistry of Ions*; Ausloos, P., Lias, S. G., Eds.; Reidel: Dordrecht, 1987; pp 97–164.

(64) Armentrout, P. B.; Simons, J. *J. Am. Chem. Soc.* **1992**, *114*, 8627.

(65) Kickel, B. L.; Armentrout, P. B. In *Organometallic Ion Chemistry*; Freiser, B. S., Ed.; Kluwer: Dordrecht, 1996; pp 1–45.

(66) Sugar, J.; Corliss, C. *J. Phys. Chem. Ref. Data* **1985**, *14*, Suppl. No. 2.

(67) On the basis of the frequencies calculated in ref 56 (57) for  $C_2H_4$  and  $M^+(C_2H_4)$ ,  $D_e - D_0 = 0.014$  (0.051) eV for  $Ti - Mn$  ( $Fe - Cu$ ).

(68) Bauschlicher, C. W., Jr.; Langhoff, S. R.; Partridge, H. In *Organometallic Ion Chemistry*; Freiser, B. S., Ed.; Kluwer: Dordrecht, 1996; pp 47–87.

**Table 3.**  $M^+(C_2H_4)$  Thermochemistry (in eV)

| M  | this study                   | theory <sup>a</sup>  | adj theory <sup>b</sup> | other labs   | our labs   |
|----|------------------------------|--|-------------------------|--|--|
| Ti | 1.51 ± 0.11                  | 1.04   | 1.34                    |  | >1.23 <sup>c,d</sup>                                   |
| V  | 1.29 ± 0.08                  | 1.08   | 1.26                    |  | 0.7 → 1.2 <sup>e</sup><br>1.20 ± 0.08 <sup>f</sup>     |
| Cr | 0.99 ± 0.11                  | 0.94   | 1.13                    |  | ≥1.3 ± 0.2 <sup>g</sup>                                |
| Mn | 0.94 ± 0.12                  | 0.68   | 0.87                    |  |  |
| Fe | 1.50 ± 0.11<br>[1.73 ± 0.11] | 1.06   | 1.30                    | 1.40 ± 0.09 <sup>h</sup><br>1.52 ± 0.22 <sup>f</sup> | 1.50 ± 0.06 <sup>d</sup><br>[1.73 ± 0.06] <sup>j</sup> |
| Co | 1.93 ± 0.09                  | 1.53<br>1.90 <sup>n</sup>  | 1.73                    | 1.82 ± 0.22 <sup>k,l</sup>                           | >1.65 ± 0.20 <sup>m</sup><br>1.86 ± 0.07 <sup>o</sup>  |
| Ni | 1.89 ± 0.11                  | 1.58   | 1.78                    | 1.91 ± 0.22 <sup>k</sup>                             | >1.43 ± 0.21 <sup>m</sup>                              |
| Cu | 1.82 ± 0.14                  | 1.51<br>1.97–2.16 <sup>q</sup><br>1.87, <sup>r</sup> 1.82 <sup>s</sup> | 1.73                    | >1.21 ± 0.04 <sup>p</sup><br>1.91–2.17 <sup>q</sup>  | >0.98 ± 0.11 <sup>m</sup>                              |

<sup>a</sup> Theory adjusted to 0 K, ref 15 except as noted. <sup>b</sup> Adjusted theory values, ref 68. See text. <sup>c</sup> Exothermic reaction, ref 33. <sup>d</sup> Reference 65. <sup>e</sup> Endothermic reaction, ref 34. <sup>f</sup> Endothermic reaction, ref 31. <sup>g</sup> Endothermic reaction, but product may not be  $Cr^+(C_2H_4)$ , see text. Reference 35. <sup>h</sup> Estimate from ref 27. See text. Adjusted from 298 K value. <sup>i</sup> KERD, ref 24. <sup>j</sup> CID, ref 20. <sup>k</sup> KERD, ref 22. Adjusted from 298 K value. <sup>l</sup> KERD, ref 25. <sup>m</sup> Endothermic reaction, ref 19. <sup>n</sup> Reference 16. <sup>o</sup> CID, ref 9. <sup>p</sup> Exothermic reaction, ref 29. <sup>q</sup> Bracketing equilibrium, ref 17. <sup>r</sup> Reference 18. Unknown whether this value is  $D_e$  or  $D_0$ . <sup>s</sup> Reference 14.

eV below (80 ± 9%) our experimental values. This comparison uses our adjusted value for the Fe BDE. The unadjusted value shows a difference from theory of 0.67 eV, a much larger discrepancy than for any other metal. Note that adjustment of our BDE for  $Ti^+(C_2H_4)$  by the  $^2F-^4F$  excitation energy would lead to a value of 0.94 ± 0.11 eV, below the theoretical  $D_0$  and in contrast to all other metals. Even better agreement is obtained for the adjusted  $D_0$  theoretical values, which are 0.09 ± 0.11 eV lower (95 ± 9%) than our experimental values. Again the adjusted Fe BDE is used for comparison because the unadjusted value has a difference of 0.43 eV. Even though there are some differences in the absolute magnitudes of the theoretical and experimental bond energies, the agreement regarding the periodic trends in the BDEs is very good and provides confidence in both sets of numbers.

The systematic difference between our results and the unadjusted theoretical values can be rationalized if the lower level of theory used to calculate the geometry of these complex cations leads to metal–ethene bond lengths that are too long and thus bond energies that are too low. Evidence supporting this idea comes from calculations of Perry<sup>16</sup> and Hertwig et al.<sup>17</sup> Perry performed calculations on the  $Co^+(C_2H_4)$  species with the geometry optimization at a higher level of theory. He obtains a  $Co^+-C_2H_4$  bond length of 2.02 Å compared with 2.31 Å calculated by Sodupe and Bauschlicher. His  $D_0$  value of 1.90 eV (adjusted from a calculated  $D_e$  value of 1.95 eV using a zero-point vibrational energy based on calculations by Bärtsch and Schwarz)<sup>57</sup> is in excellent agreement with our experimental value of 1.93 ± 0.09 (Table 3). Hertwig et al. studied  $Cu^+(C_2H_4)$  and also used higher levels of theory for their geometry optimization. They obtained a  $Cu^+-C_2H_4$  bond length of 2.016–2.098 Å compared with the 2.25 Å value calculated by SBLP. The 0 K bond energy calculated using a CCSD(T) level of theory (MP2 geometry) was 1.97 eV while B3LYP density functional methods gave 2.16 eV. (Other calculations at the MP2 and LDA/BP levels gave higher values which were discounted by these authors.) These values are slightly higher but consistent with other calculations cited in this work of 1.87<sup>18</sup> and  $D_0 = 1.82$ <sup>14</sup> eV. The 1.82 eV BDE was obtained by using a CCSD(T)/III calculation on an MP2 optimized geometry.

These latter calculations are in particularly good agreement with the BDE that we measure experimentally, 1.82 ± 0.14 eV (Table 3).

**(2) Comparison with Experiment.** Comparisons of BDEs obtained in this study can also be made with previous experimental work performed in our laboratories<sup>9,19–21,31–35</sup> and work done by others.<sup>22–30</sup> Early work performed in our laboratories has been reevaluated to include proper consideration of internal energies and is compiled elsewhere.<sup>65</sup> All these values can be found in Table 3.

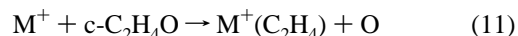
For the early metal ions, there are few experimental values available. The observation of exothermic dehydrogenation of ethane by  $Ti^+$ , reaction 10,



indicates that  $D_0(Ti^+-C_2H_4) > 1.23$  eV,<sup>30,65</sup> in agreement with the 1.51 ± 0.11 eV value determined here and contradicting the value adjusted for the  $^2F-^4F$  excitation energy of 0.94 ± 0.11 eV. This conclusively shows that the CID process for  $Ti^+(C_2H_4)$  is an adiabatic one. We also note that our BDE value is close to a recent measurement of van Koppen et al. for  $Ti^+$ -(propene), 1.49 ± 0.13 eV.<sup>69</sup>

Our previous determinations of the  $V^+(C_2H_4)$  BDE are also based on reaction 10. In early work, Aristov and Armentrout (AA)<sup>34</sup> found that vanadium cations produced by surface ionization (SI) reacted with ethane to form  $V^+(C_2H_4)$  in a barrierless, exothermic reaction. The dependence on the SI filament temperature demonstrated that this reactivity was due to excited states of  $V^+$ , as later definitively demonstrated by Hanton, Sanders, and Weisshaar.<sup>36</sup> Extrapolation of this filament temperature dependence to zero-excited-state population gave a  $V^+(C_2H_4)$  cross section that showed endothermic behavior. The estimated threshold for this process corresponds to a vanadium–ethene cation bond energy of 0.7–1.2 eV. This was believed to be too small on the basis of a comparison with other metal cation–ethene complexes available at the time (mainly those for late transition metals that have higher BDEs). AA then estimated that the  $V^+-C_2H_4$  BDE should be comparable to that of  $V^+-C_2H_2$ , determined to be ~2.17 eV in the same study. Work in progress in our laboratories has revisited this system and examined the reactions of pure ground-state vanadium cations with ethane.<sup>31</sup> Results for the dehydrogenation channel are in good agreement with the extrapolated cross sections determined by AA but provide data that can be analyzed much more definitively. The threshold for this process leads to a value for the vanadium ion–ethene bond energy of 1.20 ± 0.08 eV, in excellent agreement with the BDE obtained in this study. This demonstrates that this reaction is truly endothermic with no barrier in excess of the endothermicity, in contrast to the conclusions of AA. We also note that our BDE value is comparable to that measured by van Koppen et al. for  $V^+$ -(propene), 1.33 ± 0.09 eV.<sup>69</sup>

$Cr^+$  reacts with ethylene oxide in an endothermic process to yield a product at mass 80 amu, possibly  $Cr^+(C_2H_4)$  or  $Cr^+$ -(CO). If this is reaction 11, the measured threshold can be



interpreted to yield a  $Cr^+-C_2H_4$  BDE of 1.30 ± 0.22 eV.<sup>35</sup> This value is well in excess of the 0.99 ± 0.11 eV value determined here, which indicates that the product is probably

(69) van Koppen, P. A. M.; Bowers, M. T.; Haynes, C. L.; Armentrout, P. B. *J. Am. Chem. Soc.* Submitted for publication.

CrCO<sup>+</sup>. Indeed, the threshold measured for production of mass 80,  $2.26 \pm 0.2$  eV, is in excellent agreement with the known thermochemistry for formation of CrCO<sup>+</sup> + CH<sub>2</sub> + H<sub>2</sub>,  $2.33 \pm 0.05$  eV.<sup>40</sup> No previous values are available for Mn<sup>+</sup>(C<sub>2</sub>H<sub>4</sub>).

More extensive results are available in the literature for the late first-row transition-metal ion–ethene complexes. Previous collision-induced dissociation studies have been performed for iron and cobalt ion complexes with ethene. The values reported previously,  $D_0(\text{Fe}^+-\text{C}_2\text{H}_4) = 1.73 \pm 0.11$  eV<sup>20</sup> (uncorrected diabatic value) and  $D_0(\text{Co}^+-\text{C}_2\text{H}_4) = 1.86 \pm 0.07$  eV,<sup>19</sup> agree well with the present determinations. The previous cobalt value is slightly lower because threshold values obtained without explicit consideration of the low-energy feature were included in the final value cited. Other measurements of  $D_0(\text{M}^+-\text{C}_2\text{H}_4)$  where M = Fe,<sup>24,25,30</sup> Co,<sup>22,25,30</sup> and Ni<sup>22,70</sup> come from studies of kinetic energy release distributions (KERDs) conducted by Bowers, Beauchamp, and co-workers. The BDEs determined in the present study agree nicely with the values obtained from the KERD studies which have conservatively large uncertainties (Table 3). We also note that these studies find that the Fe BDE is 0.3–0.4 eV lower than those for Co and Ni. Presumably, the relative errors in these measurements should be smaller than the absolute uncertainties of 0.22 eV. On the basis of our measured BDEs for Co and Ni, both about  $1.9 \pm 0.1$  eV, this points to an Fe<sup>+</sup>–C<sub>2</sub>H<sub>4</sub> bond energy of 1.5–1.6 eV, consistent with our value after adjusting for the <sup>4</sup>F–<sup>6</sup>D excitation energy. This is only suggestive, however, as the measured threshold of  $1.73 \pm 0.11$  eV is still within experimental error of such an estimate.

Less direct determinations of several of these bond energies have also been made. It has been noted that Co<sup>+</sup> and Ni<sup>+</sup> fail to undergo reaction 10 (suggesting that  $D_0(\text{M}^+-\text{C}_2\text{H}_4) < 1.34$  eV or  $D_{298}(\text{M}^+-\text{C}_2\text{H}_4) < 1.41$  eV) and that the exothermic reaction 12 was observed for Co<sup>+</sup> and Ni<sup>+</sup> (suggesting that  $D_0(\text{M}^+-\text{C}_2\text{H}_4) > 1.45$  eV or  $D_{298}(\text{M}^+-\text{C}_2\text{H}_4) > 1.54$  eV).<sup>26,28</sup> It



was concluded that the metal ion–alkene bond energies exceeded 1.54 eV but not by much, hence  $D_{298}(\text{M}^+-\text{C}_2\text{H}_4) = 1.60 \pm 0.09$  eV was assigned for M = Co and Ni.<sup>26,28</sup> In truth, these observations definitively show only that  $D_0(\text{M}^+-\text{C}_2\text{H}_4) > 1.45$  eV, and this assumes that no excited electronic states are involved in the observed reactivity and does not account for the internal energy of the hydrocarbon reactant. These lower limits are in good agreement with the present determinations. Similar arguments were made by Jacobson and Freiser<sup>27</sup> for the iron ion–ethene complex. Coupled with a comparison with a 298 K Fe<sup>+</sup>–C<sub>3</sub>H<sub>6</sub> BDE of  $1.60 \pm 0.09$  eV determined from the reactions of Fe<sup>+</sup> with cyclopentane and cyclohexane, these authors estimated  $D_{298}(\text{Fe}^+-\text{C}_2\text{H}_4)$  as  $1.47 \pm 0.09$  eV which can be adjusted to  $D_0(\text{Fe}^+-\text{C}_2\text{H}_4) = 1.40 \pm 0.09$  eV. This value is in good agreement with the present determination.

Fisher and Armentrout examined the endothermic reactions 13 with M = Co, Ni, and Cu.<sup>19</sup> If the thresholds for these



reactions occur at their thermodynamic limit, then M<sup>+</sup>–C<sub>2</sub>H<sub>4</sub> bond energies of  $1.65 \pm 0.20$ ,  $1.43 \pm 0.21$ , and  $0.98 \pm 0.11$  eV, respectively, would be obtained. However, competition with much more favorable reactions (particularly formation of

MCH<sub>2</sub><sup>+</sup> + C<sub>2</sub>H<sub>4</sub>) is believed to raise the apparent thresholds for reactions 13, such that these values should be regarded as lower limits. As such, they are consistent with the present determinations. For the Cu<sup>+</sup>–C<sub>2</sub>H<sub>4</sub> complex, Burnier, Byrd, and Freiser<sup>29</sup> studied the thermal reactions of Cu<sup>+</sup> with a plethora of large esters. On the basis of the observations of exothermic pathways, they obtained a lower limit to  $D(\text{Cu}^+-\text{C}_2\text{H}_4)$  of  $1.21 \pm 0.04$  eV, also consistent with the present determination.

A more definitive estimate of this bond energy comes from work of Hertwig et al.<sup>17</sup> who examined ligand exchange equilibria of Cu<sup>+</sup> with H<sub>2</sub>O, NH<sub>3</sub>, and C<sub>2</sub>H<sub>4</sub>. They were able to bracket the Cu<sup>+</sup>–C<sub>2</sub>H<sub>4</sub> BDE as lying between  $D_0(\text{Cu}^+-\text{H}_2\text{O}) = 1.63 \pm 0.08$  eV<sup>71</sup> and  $D_0(\text{Cu}^+-\text{NH}_3)$ , which we have recently measured as  $2.46 \pm 0.16$  eV.<sup>72</sup> Because no equilibria could be established at room temperature, it was estimated that the difference in BDEs was at least 0.26 eV, which means that  $1.89 \pm 0.08$  eV <  $D_0(\text{Cu}^+-\text{C}_2\text{H}_4) < 2.20 \pm 0.10$  eV. (Hertwig et al. gave the range as 1.91–2.17 eV based on theoretical results for CuNH<sub>3</sub><sup>+</sup> and numbers rounded to the nearest kcal/mol.) Our measured value correctly predicts that  $D_0(\text{Cu}^+-\text{H}_2\text{O}) < D_0(\text{Cu}^+-\text{C}_2\text{H}_4) < D_0(\text{Cu}^+-\text{NH}_3)$ ; however, we find a difference between the Cu<sup>+</sup>–H<sub>2</sub>O and Cu<sup>+</sup>–C<sub>2</sub>H<sub>4</sub> bond energies of  $0.19 \pm 0.16$  eV, comparable to the 0.26 eV estimated as a minimum difference by Hertwig et al. However, the only products detected at long times were the multiply ligated complexes of Cu<sup>+</sup>(H<sub>2</sub>O)(C<sub>2</sub>H<sub>4</sub>) and Cu<sup>+</sup>(C<sub>2</sub>H<sub>4</sub>)<sub>2</sub>, which could mean that efficient condensation reactions suppressed observation of the singly ligated Cu<sup>+</sup>(H<sub>2</sub>O) species.

**Bond Energies for M<sup>+</sup>(C<sub>2</sub>H<sub>4</sub>)<sub>2</sub>.** Results of analyzing the product ion cross sections using eq 1 for M<sup>+</sup>(C<sub>2</sub>H<sub>4</sub>)<sub>2</sub> can be found in Table 2. Very little previous work has been done to determine thermochemistry for the bis-ligated complexes. Indeed, the only numbers in the literature appear to be estimates made by Hanratty et al. for the sum of the 298 K BDEs of the cobalt and nickel–bis-ethene complexes, 3.8 and 3.9 eV, respectively.<sup>22</sup> Adjustments to 0 K lower these values by only about 0.03 eV. These 0 K estimates are in reasonable agreement with the 0 K thermochemistry measured here, bond energy sums of  $3.51 \pm 0.17$  and  $3.68 \pm 0.19$  eV, respectively.

We now need to consider the question of whether the thresholds measured in the vanadium and manganese cases correspond to adiabatic or diabatic dissociation. For Mn<sup>+</sup>(C<sub>2</sub>H<sub>4</sub>)<sub>2</sub>, the threshold measured for the loss of ethene is higher than that for all other metal–bis-ethene complexes studied here. This is an unexpected result given that the LM<sup>+</sup>–L BDE for M = Mn is the weakest among all first-row transition–metal ions for other ligands, L = H<sub>2</sub>O<sup>51</sup> and CO.<sup>38–45</sup> However, if the threshold energy measured is for diabatic (spin-allowed) dissociation, the adiabatic BDE is obtained by reducing the measured threshold by the septet–quintet excitation energy for Mn<sup>+</sup>(C<sub>2</sub>H<sub>4</sub>), 1.0 eV as calculated by SBLP.<sup>15</sup> Given an estimated uncertainty in this excitation energy of 0.1 eV, the adiabatic BDE then would be  $0.91 \pm 0.15$  eV (Table 4). In the case of V<sup>+</sup>(C<sub>2</sub>H<sub>4</sub>)<sub>2</sub>, if the BDE measured in this study corresponded to diabatic instead of adiabatic dissociation, the measured threshold would need to be corrected by the quintet–triplet excitation energy for V<sup>+</sup>(C<sub>2</sub>H<sub>4</sub>),  $0.64 \pm 0.1$  eV as calculated by SBLP (uncertainty estimated).<sup>15</sup> The adiabatic BDE would be  $0.68 \pm 0.17$  eV. Further discussion of both of these potential corrections is found below.

(71) Dalleska, N. F.; Honma, K.; Sunderlin, L. S.; Armentrout, P. B. *J. Am. Chem. Soc.* **1994**, *116*, 3519.

(72) Walter, D.; Armentrout, P. B. *J. Am. Chem. Soc.* Submitted for publication.

(70) The 298 K BDE has been adjusted to 0 K consistent with the conversions suggested in ref 65.

**Table 4.** Comparison of BDE of  $ML^+$  and  $ML_2^+$  ( $L = CO, C_2H_4$ )

| M  | $ML^+$            |                   | $ML_2^+$          |                     |
|----|-------------------|-------------------|-------------------|---------------------|
|    | CO                | $C_2H_4^a$        | CO                | $C_2H_4^a$          |
| Ti | $1.22 \pm 0.01^b$ | $1.51 \pm 0.11$   | $1.17 \pm 0.04^b$ |                     |
| V  | $1.17 \pm 0.03^c$ | $1.29 \pm 0.08$   | $0.94 \pm 0.04^c$ | $1.32 \pm 0.14$     |
| Cr | $0.93 \pm 0.04^d$ | $0.99 \pm 0.11$   | $0.98 \pm 0.03^d$ | $1.12 \pm 0.11$     |
| Mn | $0.26 \pm 0.10^e$ | $0.94 \pm 0.12$   | $0.65 \pm 0.10^e$ | $1.91 \pm 0.11$     |
|    |                   |                   |                   | $[0.91 \pm 0.15]^f$ |
| Fe | $1.36 \pm 0.08^g$ | $1.50 \pm 0.11^f$ | $1.57 \pm 0.15^g$ | $1.57 \pm 0.16$     |
| Co | $1.80 \pm 0.07^h$ | $1.93 \pm 0.09$   | $1.58 \pm 0.09^h$ | $1.58 \pm 0.14$     |
| Ni | $1.81 \pm 0.11^i$ | $1.89 \pm 0.11$   | $1.74 \pm 0.11^i$ | $1.79 \pm 0.15$     |
| Cu | $1.54 \pm 0.07^j$ | $1.82 \pm 0.14$   | $1.78 \pm 0.03^j$ | $1.80 \pm 0.13$     |

<sup>a</sup> Taken from Table 2. <sup>b</sup> Reference 38. <sup>c</sup> Reference 39. <sup>d</sup> Reference 40. <sup>e</sup> Reference 41. <sup>f</sup> Adiabatic value from Table 3. <sup>g</sup> Reference 42. <sup>h</sup> Reference 43. <sup>i</sup> Reference 44. <sup>j</sup> Reference 45.

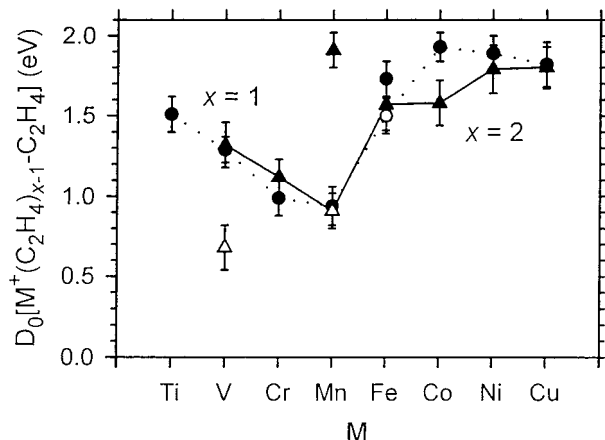


**Figure 3.** Bond dissociation energies in eV for the first-row transition-metal cation mono-ethene (circles) and bis-ethene (triangles) complex cations. In all cases, solid symbols correspond to the directly measured BDEs. Open symbols correspond to values adjusted by the excitation energy of the product. The most likely adiabatic BDEs are connected by lines.

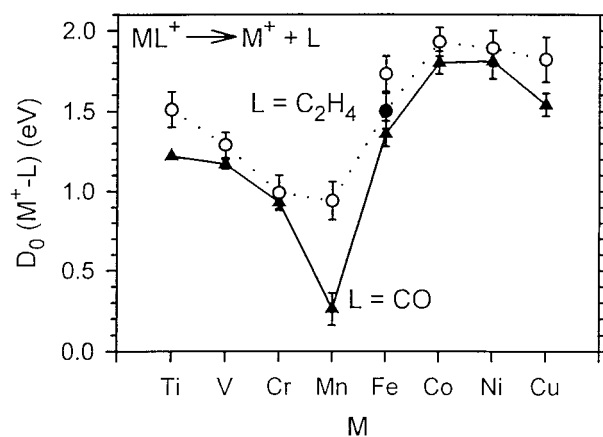
#### Periodic Trends in Metal Ion–Ethene Thermochemistry.

Figure 3 shows the bond energies of the mono- and bis-ligated transition-metal complexes with ethene. Solid symbols correspond to directly measured values, while open symbols for  $Fe^+(C_2H_4)$ ,  $V^+(C_2H_4)_2$ , and  $Mn^+(C_2H_4)_2$  refer to values adjusted for possible diabatic dissociation. For the mono-ligated complexes, the BDEs decrease smoothly from Ti to Mn and Co to Cu. From Mn to Co, there is a large increase in the BDEs. The decreases observed for the early and late metals can be attributed to the increased occupation of d orbitals that have antibonding character.

For the bis-ligated complexes of Cr and Fe–Cu, the second BDEs are comparable to those of the mono-ligated complexes. Although this result is not a necessary one, in the two cases where there is the question of adiabatic vs diabatic dissociation, V and Mn, the first and second BDEs also agree nicely if the adjustment for excitation energy is made in the latter case, but not in the former. This gives supporting evidence that the true adiabatic BDE of  $V^+(C_2H_4)_2$  is directly measured while  $Mn^+(C_2H_4)_2$  dissociates diabatically such that the adiabatic BDE is determined by correcting the measured threshold for the excitation energy of the mono-ethene complex cation.

#### Comparison of Ethene and Carbonyl Bond Energies.

In Figures 4 and 5, we compare the periodic trends observed for the isobaric ethene and carbonyl<sup>38–45</sup> complexes of the first-row transition-metal cations. For both the mono- and bis-ligated systems, the periodic trends are similar for both the CO and  $C_2H_4$  systems. In most cases, the ethene BDEs are slightly



**Figure 4.** Adiabatic bond dissociation energies in eV for the first-row transition-metal cation mono-ligated complexes with ethene (circles) and carbon monoxide (solid triangles). Open circles correspond to the directly measured BDEs. Solid circles correspond to values adjusted by the excitation energy of the product. The most likely adiabatic BDEs are connected by lines.

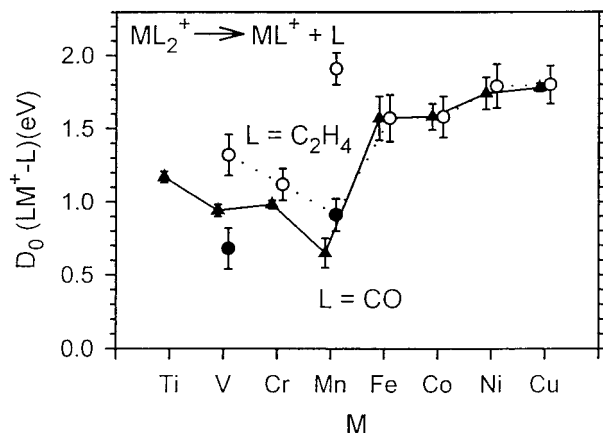


**Figure 5.** Adiabatic bond dissociation energies in eV for the first-row transition-metal cation bis-ligated complexes with ethene (open circles) and carbon monoxide (solid triangles). Open circles correspond to the directly measured BDEs. Solid circles correspond to values adjusted by the excitation energy of the product. The most likely adiabatic BDEs are connected by lines.

greater, which may be a result of the higher polarizability of ethene ( $4.10 \text{ \AA}^3$ ) vs that of CO ( $1.94 \text{ \AA}^3$ )<sup>73</sup> allowing a stronger electrostatic interaction. Note that this agreement again suggests that the  $Mn^+(C_2H_4)_2$  BDE needs to be corrected. The comparison for  $V^+(C_2H_4)_2$  is more ambiguous, although the uncorrected number is favored by noting that it seems unlikely that this system would be the only case where the ethene BDE fell below that for the carbonyl.

For both mono-ligated systems, the largest BDE occurs for the cobalt cation. The  $Ti^+(C_2H_4)$  BDE is somewhat greater than that of  $Ti^+(CO)$ , which can probably be attributed to the covalent character of bonding in the former species.<sup>15</sup> In this regard, we note that SBLP found that the electrostatically bound  $Ti^+(C_2H_4)$  species lay 0.23 eV above the ground-state covalently bound complex, comparable to the 0.29 eV difference in BDEs between the CO and  $C_2H_4$  ligands. The large difference observed in the two systems for the case of  $Mn^+$  is particularly interesting. This is the only first-row transition-metal ion where the ligated complex has the metal 4s orbital occupied. We speculate that because the donor orbital on ethene (the C–C  $\pi$

(73) Rothe, E. W.; Bernstein, R. B. *J. Chem. Phys.* **1959**, *31*, 1619.



orbital) is more diffuse than that on CO (the C lone pair), there is a weaker repulsive interaction with the 4s electron in the former case.

**Comparison with Other Ligands.** In addition to the carbonyls, systematic BDEs for  $\text{NH}_3$ <sup>72</sup> and  $\text{H}_2\text{O}$ <sup>51</sup> with the first-row transition-metal cations have been obtained previously. As recently pointed out,<sup>72</sup> the  $\pi$ -bonding character of these ligands can be investigated by comparing the average BDEs of the first and second ligands bound to the early metals (Ti–Cr) vs those to the late metals (Co–Cu). This comparison shows an increase of 16% in the BDEs to  $\text{H}_2\text{O}$ , a 32% increase for  $\text{NH}_3$ , and a 61% increase for CO. The present data shows that there is a 53% increase for the  $\text{C}_2\text{H}_4$  ligand. In the case of  $\text{NH}_3$ , it can be shown that the increase correlates nicely with the increased electrostatic interaction between the metal and the ligand as the radius of the ion decreases with increasing nuclear charge.<sup>74</sup> All metal ligand complexes should show this effect, so changes differing from a 32% increase indicate other factors at work. For  $\text{H}_2\text{O}$ , the lower increase can be attributed to the  $\pi$ -donor ability of this ligand. This is advantageous for the early metals that can accept electron density into empty  $3d\pi$  orbitals and disadvantageous for the late metals which must occupy the  $3d\pi$  orbitals. The increases observed for ethene and CO, both  $\pi$ -acceptors, can be attributed to  $3d\pi$  back-donation into the

(74) Bauschlicher, C. W., Jr.; Langhoff, S. R.; Partridge, H. *J. Chem. Phys.* **1991**, *94*, 2068.

antibonding ligand orbitals. The late metals can have doubly occupied  $3d\pi$  orbitals enhancing this interaction compared to the early metals which have only singly occupied  $3d\pi$  orbitals. CO exhibits a slightly stronger effect than ethene because it can accept  $\pi$  electrons in two orbitals rather than just one.

Another indication of the influence of  $\pi$ -back-bonding comes from a comparison of the BDEs of the first and second ligand to the metal cation. For the late metals, Co–Cu, the second  $\text{NH}_3$  ligand is more strongly bound than the first while the second ethene ligand is bound more weakly than the first. For  $\text{NH}_3$ , this effect was explained<sup>72,74</sup> by the energetic requirements associated with  $s$ – $d\sigma$  hybridization which are largely paid by the first metal–ligand bond, thereby allowing the second ligand to benefit with little additional energy required. Although a similar effect is probably playing a role in the ethene systems, two ethene ligands must also share the  $3d\pi$  back-bonding electrons such that the back-bonding interaction is weaker for the doubly ligated systems compared to the singly ligated systems.

**Acknowledgment.** This work is supported by NSF Grant No. CHE-9530412. We also thank NSF for funding under the auspices of the REU program. We thank S. Bärsch, H. Schwarz, R. H. Hertwig, and W. Koch for providing the results of their theoretical calculations to us.

JA973834Z